

On a simple way to calculate electronic resonances for polyatomic molecules

J. Horáček, I. Paidarová, and R. Čurík

Citation: *The Journal of Chemical Physics* **143**, 184102 (2015); doi: 10.1063/1.4935052

View online: <http://dx.doi.org/10.1063/1.4935052>

View Table of Contents: <http://scitation.aip.org/content/aip/journal/jcp/143/18?ver=pdfcov>

Published by the [AIP Publishing](#)

Articles you may be interested in

[Accurate ab initio potential energy surface, thermochemistry, and dynamics of the \$F^- + CH_3F\$ SN2 and proton-abstraction reactions](#)

J. Chem. Phys. **142**, 244301 (2015); 10.1063/1.4922616

[Negative ions of p-nitroaniline: Photodetachment, collisions, and ab initio calculations](#)

J. Chem. Phys. **138**, 234304 (2013); 10.1063/1.4810869

[Correlated complex independent particle potential for calculating electronic resonances](#)

J. Chem. Phys. **123**, 204110 (2005); 10.1063/1.2130338

[Four-mode quantum calculations of resonance states in complex-forming bimolecular reactions: \$Cl^- + C_2H_3Br\$](#)

J. Chem. Phys. **122**, 234306 (2005); 10.1063/1.1924406

[Four-mode calculation of resonance states of intermediate complexes in the SN2 reaction \$Cl^- + CH_3Cl \rightarrow ClCH_3 + Cl^-\$](#)

J. Chem. Phys. **118**, 4499 (2003); 10.1063/1.1541626



AIP | APL Photonics

APL Photonics is pleased to announce
Benjamin Eggleton as its Editor-in-Chief



On a simple way to calculate electronic resonances for polyatomic molecules

J. Horáček,^{1,a)} I. Páidarová,² and R. Čurík^{2,b)}

¹Faculty of Mathematics and Physics, Charles University, V Holešovičkách 2, 18000 Praha 8, Czech Republic

²J. Heyrovský Institute of Physical Chemistry, Academy of Sciences of the Czech Republic, v.v.i., Dolejškova 3, 182 23 Prague 8, Czech Republic

(Received 24 June 2015; accepted 21 October 2015; published online 9 November 2015)

We propose a simple method for calculation of low-lying shape electronic resonances of polyatomic molecules. The method introduces a perturbation potential and requires only routine bound-state type calculations in the real domain of energies. Such a calculation is accessible by most of the free or commercial quantum chemistry software. The presented method is based on the analytical continuation in a coupling constant model, but unlike its previous variants, we experience a very stable and robust behavior for higher-order extrapolation functions. Moreover, the present approach is independent of the correlation treatment used in quantum many-electron computations and therefore we are able to apply Coupled Clusters (CCSD-T) level of the correlation model. We demonstrate these properties on determination of the resonance position and width of the ${}^2\Pi_u$ temporary negative ion state of diacetylene using CCSD-T level of theory. © 2015 AIP Publishing LLC. [<http://dx.doi.org/10.1063/1.4935052>]

I. INTRODUCTION

Molecular resonances (temporary molecular anions) play an important role in processes that involve nuclear dynamics, i.e., vibrational excitation, dissociative attachment, and associative detachment. Resonances are defined as poles of the S-matrix lying on the unphysical energy sheet, or as eigenstates of the physical Hamiltonian with the Siegert boundary condition.¹ The energy eigenvalues are generally complex $E = E_R - i\Gamma/2$ where E_R is the resonance energy and Γ is the resonance width determining the lifetime of the temporary negative ion (TNI) state. Several methods were developed to calculate the energies and widths of real molecules based on stabilization procedures,² or the complex scaling approach.³ In comparison with the calculation of bound states, these methods are computationally very demanding.

Recently, a method originally proposed in the field of nuclear physics—the method of analytical continuation in coupling constant (ACCC)^{2,4,5}—has been applied with considerable success to molecular anions: nitrogen⁶ N_2 , valine, glycine, adenine, formic acid, dimer of formic acid,⁷ ethylene,⁸ and carbon dioxide⁹ CO_2 . The ACCC method is based on the introduction of a perturbation potential which transforms resonance states into bound states. An attractive short-range interaction U multiplied by a real positive parameter λ (coupling constant) is added to the original Hamiltonian H ,

$$H \rightarrow H + \lambda U = H_\lambda. \quad (1)$$

At increasing λ , the new Hamiltonian H_λ gets more attractive and some resonance states eventually transform into bound states. Calculation of the bound state energies and their square integrable wave functions is now a routine task even for large

polyatomic molecules and many commercial programs are available. A set of bound state affinities $E_i = -\kappa_i^2$ calculated at points λ_i may be easily obtained. As soon as the calculated energies are available, the next step is to analytically continue the energy into a complex plane for $\lambda \rightarrow 0$. The process of analytical continuation is however a very complicated task. It is well known that extrapolation and continuation are ill-conditioned procedures and high accuracy of the data is usually required.

The analytical continuation is routinely carried out by construction of a Padé approximation¹⁰ (PA), i.e., by representing the continued function as a ratio of two polynomials. This approach, however, provides very unstable results at increasing orders of PA. Higher PA approximations are often defective, e.g., they locate resonances on the physical sheet, or they produce poles at real and positive energies. Moreover, very often so-called Froissart doublets, i.e., pairs of defective poles and near zeros, are formed.¹¹ Such approximations should be discarded as unphysical but it is very difficult to avoid them. The appearance of a defective PA indicates that the class of functions used in the construction of the PA is too broad and it should be restricted.

The present method is based on a new variant of the ACCC method which keeps all advantages of the original ACCC method but which improves significantly the stability of the original approach. It differs from the direct ACCC in the sense that the function analytically continued into the complex plane is the function $\lambda(\kappa)$ proper, where the momentum k is written as $k = i\kappa$ (not the function $\kappa(\lambda)$ as in the original ACCC method). The improvement in stability is achieved by introducing physical constraints on PA used to represent the function $\lambda(\kappa)$.

We intend to demonstrate the applicability of the method on a diacetylene molecule. The diacetylene is a rather unusual molecule—relatively long and linear, carbon-rich system with

^{a)}Electronic mail: horacek@mbox.troja.mff.cuni.cz

^{b)}Electronic mail: roman.curik@jh-inst.cas.cz

energetic bonds. Diacetylene was detected in the interstellar space and upper layers of planetary atmospheres^{12,13} (Uranus and Titan). It is also known to be an intermediate in the formation of soot in flames.^{14,15} An interest from these fields motivated several theoretical and experimental studies devoted to the investigation of low-energy collisions of electrons with diacetylene. A dominant feature appearing in vibrationally inelastic collisions is the ${}^2\Pi_u$ resonance that was first observed around 1 eV in transmission experiments.¹⁶ Later, cross-beam experiments¹⁷ confirmed a boomerang structure of resonant excitation for several resolved vibrational modes with reported autodetachment widths of 30 meV. Electron-impact vibrational excitation was also computed by employing the Discrete Momentum Representation (DMR) method.¹⁸ The ${}^2\Pi_u$ resonance is very clearly positioned in their inelastic cross sections at 1.33 eV. A joint theoretical and experimental study focused on elastic collisions of electrons with diacetylene¹⁹ reported a calculated value of the ${}^2\Pi_u$ resonance energy as 0.5 eV. Two more theoretical methods were employed to determine fixed-nuclei parameters of the ${}^2\Pi_u$ resonance. Results of the Single Center Expansion (SCE) and R-matrix methods are combined in a joint paper.²⁰ Both methods position the resonance at 2.2 eV with the resonance width of 0.3 eV.

The evident discrepancy among all the reported resonance parameters motivated our present attempt to study this resonance with CCSD-T level of theory and with our new method of analytical continuation described in Sec. II.

II. REGULARIZED ANALYTICAL CONTINUATION (RAC) METHOD

The new method, which we will term as the RAC in the coupling constant, proposed in this paper, is based on the inverse variant of the ACCC method, i.e., the RAC method seeks zeros of the function $\lambda(\kappa)$ in contrast to the direct ACCC approach where the inverse function $\kappa(\lambda)$ is considered. This allows us to put restrictions on the class of approximating functions used with the effect that all unphysical states are excluded. This step was not possible in the direct application of the ACCC method. The function $\lambda(\kappa)$ is subject of the following general properties:²

- $\lambda(\kappa)$ is a real function for real κ increasing at positive κ .
- It is known^{2,4,5} that for nonzero angular momentum l the function $\kappa(\lambda)$ behaves, close to the threshold $\kappa = 0$, as $\kappa(\lambda) \sim \sqrt{\lambda - \lambda_0}$. As a direct consequence, the inverse function behaves as $\lambda(\kappa) \sim \lambda_0 + b\kappa^2$ and has therefore a local minimum at the threshold $\kappa = 0$.
- For real potentials, the function $\lambda(\kappa)$ may have three types of zeros: bound states lying on the physical sheet with κ real and positive, virtual states at negative real values of κ and pairs of resonances (complex values) with imaginary part of momentum k negative, this means that in the κ -plane the real parts of κ must be negative.

Following the lines of the direct ACCC, we represent the function $\lambda(\kappa)$ in the form of Padé approximations. The simplest

PA satisfying all the conditions above is

$$\lambda^{[2/1]}(\kappa) = \lambda_0 \frac{\kappa^2 + 2\alpha^2\kappa + \alpha^4 + \beta^2}{\alpha^4 + \beta^2 + 2\alpha^2\kappa} = \lambda_0 g(\alpha, \beta; \kappa), \quad (2)$$

where α , β , and λ_0 are real parameters. This function has two complex conjugate zeros at

$$\kappa_{1,2} = -\alpha^2 \pm i\beta, \quad (3)$$

or in the k -space

$$k_{1,2} = \mp\beta - i\alpha^2, \quad (4)$$

and obviously describes one pair of resonances with the following energy and width:

$$\begin{aligned} E_r &= \beta^2 - \alpha^4, \\ \Gamma &= 4\alpha^2\beta. \end{aligned} \quad (5)$$

The parameters α and β have direct physical meaning determining the real and imaginary parts of the resonance momentum as shown in Eq. (4). The parameter λ_0 is of multiplicative nature only and does not have any real physical significance. In order to get the resonance parameters, the function has to be fitted to the input data $\{\lambda_i, \kappa_i\}$ and the resonances are determined as zeros of the function $g(\alpha, \beta; \kappa)$. In order to obtain the resonance parameters, we minimize the following functional:

$$\chi^2 = \frac{1}{N} \sum_{i=1}^N |\lambda_0 g(\alpha, \beta; \kappa_i) - \lambda_i|^2, \quad (6)$$

where N is the number of input points $\{\lambda_i, \kappa_i\}$. Determination of the parameters α , β , and λ_0 requires performing a nonlinear minimization procedure. It is well known that a good initial guess of the minimization parameters is vital for finding a realistic solution of the minimization problem. In the present case, however, the problem of choosing the initial values of the parameters is very easy and a good estimate of the starting fit values is always possible. The low-lying shape molecular resonances have their energies of the order of several eV and widths of the order of 1 eV or less. By guessing the parameters α_g and β_g from the expected position of the resonance, one can obtain the estimate for λ_0 as

$$\lambda_0 \approx \lambda_i / g(\alpha_g, \beta_g; \kappa_i) \quad (7)$$

from an i th data point $\{\lambda_i, \kappa_i\}$ arbitrarily chosen and to start the minimization process. It is remarkable to note, as will be shown later, that this simplest representation of the function $\lambda(\kappa)$, represented by Eq. (2), already gives a very reasonable description of a typical molecular resonance. In accordance with the nomenclature, we denote this approximation as PA [2/1]. In fact the number of independent parameters could be effectively reduced to two (α and β) provided at each iteration step of the minimization procedure we set

$$\lambda_0 = \lambda_i / g(\alpha, \beta; \kappa_i), \quad (8)$$

where α and β are the current values of the fitted parameters. In this case, the fit will be exact at the data point $\{\lambda_i, \kappa_i\}$.

Often the behavior $\lambda(\kappa)$ is influenced by a second pole of the scattering matrix that lies in vicinity of the examined resonance. It may be a virtual state or it may be a second

resonance. Such a presence of the second pole can be reflected by a construction of higher-order approximations. If we add one virtual state to the examined resonance, we get a [3/1] PA,

$$\lambda^{[3/1]}(\kappa) = \lambda_0 \frac{(\kappa^2 + \alpha^2\kappa + \alpha^4 + \beta^2)(1 + \delta^2\kappa)}{\alpha^4 + \beta^2 + \kappa(\alpha^2 + \delta^2(\alpha^4 + \beta^2))}. \quad (9)$$

In this case, we have one additional real parameter δ to fit. This parameter determines the energy of the virtual state as $E_v = -\delta^{-4}$. Since, as already said, the PA [2/1] is usually a very good approximation to use resonance parameters obtained at the lower level and start the minimization procedure setting $\delta = 0$. The presence of a near resonance can be reflected in a similar manner. For example, to incorporate two resonances in the fit, we can write

$$\lambda^{[4/2]}(\kappa) = \lambda_0 \frac{(\kappa^2 + \alpha^2\kappa + \alpha^4 + \beta^2)(\kappa^2 + \gamma^2\kappa + \gamma^4 + \delta^2)}{(\alpha^4 + \beta^2)(\gamma^4 + \delta^2)(1 + \mu^2\kappa)(1 + \mu^2\epsilon^2\kappa)}, \quad (10)$$

where

$$\mu^2 = \frac{1}{1 + \epsilon^2} \left(\frac{\alpha^2}{\alpha^4 + \beta^2} + \frac{\gamma^2}{\gamma^4 + \delta^2} \right). \quad (11)$$

All these functions satisfy the three conditions required above and in all cases the resonance energy is obtained as $E_R = \beta^2 - \alpha^4$ and the width as $\Gamma = 4\alpha^2|\beta|$. As in the [2/1] case (2), all the fitting parameters are real.

This outlined procedure (RAC) for construction of regularized higher-order Padé approximations is free of the stability problems we encountered in our previous studies. Different higher-order approximations can be easily constructed. In the following, we also report results for [3/2] and [4/3] that are omitted here for reasons of clarity. It is worth mentioning that in all cases the existence of the Froissart doublets (i.e., the existence of defective approximations) on the physical sheet is eliminated.

III. NOTES ON IMPLEMENTATION

In practical applications we are faced with the problem of how to choose the perturbation potential U and how to select the range of values of λ_i used for the calculation of the affinities $E_i = -\kappa_i^2$. It is supposed that the perturbation potential U must be of short range but reasonable results are often obtained even for Coulomb potential. This is caused by the fact that in quantum chemistry calculations all wave functions are represented as sums of square integrable functions reducing effectively the impact of the Coulomb tail. The Gaussian potential seems to be a good candidate but our present experience indicates that the results are sensitive to the choice of exponent of the Gaussian function. In a recent paper,⁹ Sommerfeld and Ehara studied the possibility of using the Voronoi soft-box potential as the perturbation potential in the ACCC method with very promising results. Generally, the question about the best perturbation potential is still open.

The next important consideration is the range of the values λ_i we chose for the analytical continuation. This range is tightly connected with the obtained range of the affinities E_i (see Fig. 1). The affinity energies cannot be arbitrarily

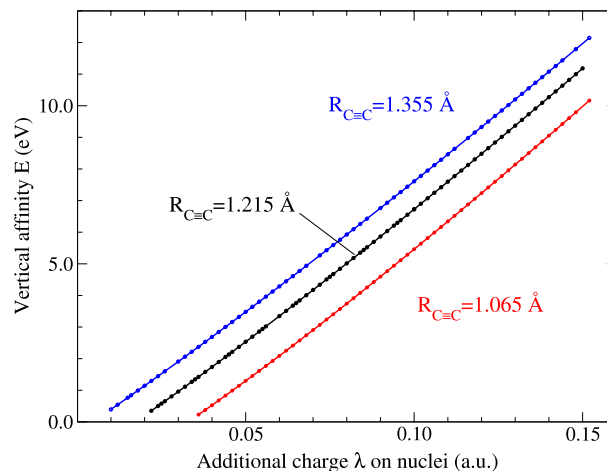


FIG. 1. Computed vertical electron affinity diacetylene $E(\lambda)$ as a function of charge parameter λ for three selected internuclear distances: equilibrium distance $R_{C=C} = 1.215$ Å (black curve), bond length elongated by 0.14 Å (blue curve), and bond length shortened by 0.15 Å (red curve).

small because the electronic wave functions with low binding energies possess a large spatial extent and thus they are harder to represent by compact Gaussian bases used in the available quantum chemistry programs. Moreover, theory dictates that use of long-range Coulomb potential for perturbation U gives rise to an infinite number of bound Rydberg states no matter how weak the Coulomb potential is. We have demonstrated⁶ that for a very weak Coulomb field these Rydberg states become preferred ground states and they may plague the data used for the analytic continuation. However, in Sec. IV we will show that these Rydberg states are very clearly identifiable on the affinity curve $E(\lambda)$ and the present theory can be successfully applied providing one avoids the low-energy part of the computed data.

On the other hand, for large λ parameters, more than one resonance may be brought from the continuum to the bound space. Thus, more poles may contribute to the function $\lambda(\kappa)$ and consequently the validity of our low-order approximations in Eqs. (2), (9), and (10) is diminished. Our experience indicates that a suitable range of selected affinities can be chosen somewhere in between 0.2 and 20 eV for systems we studied so far. The problem of choosing the optimal energy range will be discussed in our future work.

IV. QUANTUM CHEMISTRY FOR ${}^2\Pi_u$ STATE OF DIACETYLENE

Ab initio calculations for the electron affinities $E_i(\lambda_i)$ in the presence of the external Coulomb field were done using the CCSD-T method^{21,22} as implemented in the MOLPRO 10 package of quantum-chemistry programs.²³ For the basis set, we employed Dunning's augmented correlation-consistent basis of triple-zeta quality²⁴ (aug-cc-pVTZ). We obtained the following equilibrium bond distances: $R_{C-C} = 1.379$ Å, $R_{C=C} = 1.215$ Å, and $R_{C-H} = 1.064$ Å. They compare favorably with bond lengths determined experimentally:²⁵ $R_{C-C} = 1.371$ Å, $R_{C=C} = 1.210$ Å, and $R_{C-H} = 1.061$ Å. Electron affinities in the presence of the attractive Coulomb field U are

calculated as a difference between the ground state energy of the neutral molecule and ground state energy of the negative ion. The attractive Coulomb field makes certain that the ground state of the negative ion exists. In the present study, the attractive Coulomb field takes the following form:

$$\lambda U(\mathbf{r}) = - \sum_{A=1}^6 \frac{\lambda}{|\mathbf{r} - \mathbf{R}_A|}, \quad (12)$$

where \mathbf{R}_A are position vectors of all six nuclei of the diacetylene. We have chosen to evaluate the resonance parameters along the $R_{C\equiv C}$ coordinate because the ${}^2\Pi_u$ resonance exhibits an anti-bonding character with respect to the $R_{C\equiv C}$ bond and it strongly drives the resonant vibrational excitation along this bond;^{17,18} however, the $R_{C\equiv C}$ bond does not dissociate at low collision energies.²⁶ The dominant low-energy dissociative electron attachment (DEA) channel leads to an abstraction of neutral hydrogen, i.e., the dissociation fragments are $(\text{HCCCC})^- + \text{H}$. In order to compute a resonance surface along the $R_{C\equiv C}$ coordinate, we kept the molecule linear and the remaining geometry parameters (R_{C-C} and R_{C-H}) were fixed at the equilibrium values. The bond length distance $R_{C\equiv C}$ was varied evenly for both $\text{C}\equiv\text{C}$ triple bonds of diacetylene.

A typical output from the *ab initio* part of our study is shown in Fig. 1 in which we display the λ -dependence of electron affinity $E(\lambda)$ for three selected internuclear distances $R_{C\equiv C}$. The curves displayed in Fig. 1 are analytically continued to the area below the x -axis where they become complex and resonance parameters are extracted at $\lambda = 0$ as described in Eqs. (2)-(11). Results of the analytical continuation and the technical details will be given in Sec. V.

In the remaining part of this section we would like to address the present choice of Coulomb potential (12) for perturbation λU added to the molecular Hamiltonian. This choice appears to be in contradiction to a necessary short-range nature of the perturbation λU required by threshold behavior $\kappa(\lambda) \sim \sqrt{\lambda - \lambda_0}$ imposed on the continued function in Sec. II. Although these concerns were partially addressed in our previous work,⁶ they will be elaborated on in more detail here.

The method proposed in this paper makes use of a common quantum chemistry software. Most of this software employs compact basis sets (often implemented as Cartesian or spherical harmonic Gaussians). Such basis sets limit the spatial extent of the electronic wave function and effectively cut off the long-range tail of Coulomb potential (12). Exploiting the finite spatial extent of the basis set may seem to be a random or hazardous approach. It may appear that results will strongly depend on the spatial extent of the basis because no matter how small the charges λ are, there should always be an infinite number of Rydberg bound states. With a sufficiently diffuse basis set, these Rydberg states will always support the negative molecular ion, even in a case when λU is too weak to support the resonant state.

Naturally, the following question can be raised: Is it possible to separate results describing a resonant state bound by the short-range part of Coulomb field (12) (effectively cut off by the basis set) from results describing a Rydberg state? To answer this question, we repeated calculations for equilibrium

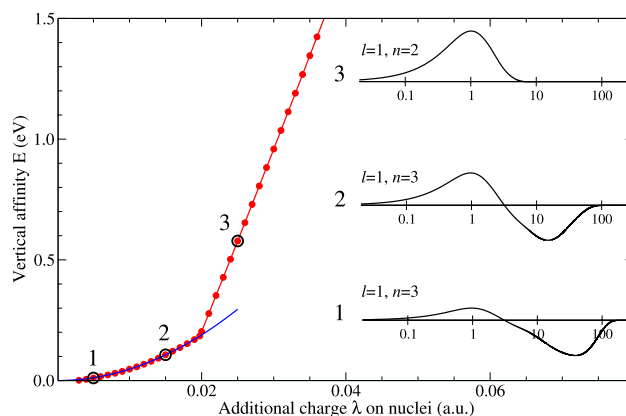


FIG. 2. Computed vertical electron affinity of diacetylene $E(\lambda)$ as a function of the charge parameter λ for equilibrium distance (red points connected with red line) with extended basis set (see the text). The blue line represents a quadratic fit $E = (6\lambda)^2/2\nu^2$. Three plots on the right side show the radial wave functions of the singly occupied molecular orbital from the reference determinant. These wave functions are displayed for the three different λ parameters shown as black circles on the affinity curve on the left. Note that due to large spatial extent of the wave functions we use logarithmic scale for the radial coordinate.

geometry (shown as a black curve in Fig. 1) employing an extended basis set. In order to describe the Rydberg states, the original aug-cc-pVTZ basis was expanded in even tempered fashion (ratio of 3.5) by four (s , p)-type functions on each of the six nuclear centers. As a result, we observed negligible energy shift for the curves displayed in Fig. 1. However, the extended basis changed results dramatically in the low energy domain not shown in Fig. 1. These results are presented in Fig. 2 as red points connected with a red line. It is clear that the affinity curve can now be separated into two very distinct regions. The region for $\lambda \gtrsim 0.02$ is practically identical with the data shown in Fig. 1 and we will call it the valence region. For the charges $\lambda \lesssim 0.02$, the Coulomb field is too weak to bind the resonance in the valence state and the curve switches to the Rydberg region. The valence curve dives into the series of Rydberg states of the same symmetry producing a series of avoided crossings. However, in the present calculations we are looking for the ground state of the system and therefore the valence curve switches to the lowest lying Rydberg state supported by our basis.

In the language of Quantum Defect Theory²⁷ (QDT), we may imagine the system in the Rydberg region of Fig. 2 as a single Rydberg electron in long-range Coulomb field (12) of the total charge 6λ , while the short-range interaction is generated by the neutral diacetylene molecule. In the QDT, the effect of the short-range interaction is incorporated into a quantum defect $\mu_l(E)$ and the energy levels of the Rydberg electron can be expressed by Mulliken's formula

$$E_{nl} = \frac{(6\lambda)^2}{2\nu_l^2}, \quad (13)$$

where the effective quantum number $\nu_l = n - \mu_l(E)$ can be considered as energy independent in the interval of Rydberg affinities displayed in Fig. 2. Hence, it is not surprising that the blue line in Fig. 2 shows an excellent agreement of quadratic function (13) fit with the computed vertical affinities.

For a more illuminating demonstration, we have also extracted the radial wave functions of a singly occupied molecular orbital from the reference determinant that enters the following coupled clusters calculations. These wave functions are plotted on the right side of Fig. 2 for three different λ parameters. First two λ parameters belong to the Rydberg domain of the affinity curve and the wave functions clearly describe the $n = 3$ Rydberg states of ${}^2\Pi_u$ symmetry (with lowest partial wave $l = 1$) extending up to 100 bohrs. The third (uppermost) wave function corresponds to the valence domain describing $n = 2$ anti-bonding π^* orbital in the ${}^2\Pi_u$ symmetry. It is important to note that angular momentum l is not a good quantum number because of the angular anisotropy of the diacetylene molecule and the effects coming from coupling of the partial waves were neglected in the present qualitative analysis.

We may conclude that with a little care even long-range Coulomb potential (12) may be applied for techniques of analytic continuation. This conclusion comes from two independent observations. First, any finite-extent basis set effectively cuts off the Coulomb tail of the potential. Second, the resulting electron affinity may belong to one of the two very distinct domains of the affinity curve $E(\lambda)$ shown in Fig. 2 and hence it is very clear to ensure that the analytic continuation is done only on the valence part of the $E(\lambda)$ curve.

V. RESULTS AND DISCUSSION

In this section we apply the proposed RAC procedure to the data discussed above. Let us first consider the resonance at the equilibrium geometry. In our case, the full set of data covers computed affinities in the energy range from 0.20 eV to 11.18 eV. In Table I, we show the resonance parameters obtained at five different levels of the RAC method. Hence, all of the Padé approximations we employed satisfy the physical properties summarized in Section II. For example, RAC [2/1], [3/1], and [4/2] are described by Equations (2), (9), and (10), respectively.

We see that in the present case the lowest PA [2/1] approximation gives resonance parameters with excellent agreement with higher order approximations. In our opinion, the PA [3/1] approximation represents the best compromise between accuracy and computational effort and we will restrict ourselves to the PA [3/1] approximation in what follows. The resulting resonance positions and widths as functions of $R_{C\equiv C}$ are summarized in Table II.

In Fig. 3, we display ${}^1\Sigma_g$ curve for the neutral ground state (black curve) together with the potential energy surface

TABLE I. Resonance energy and width of the diacetylene state ${}^2\Pi_u$ calculated at various orders of RAC at the equilibrium geometry.

RAC order	Energy E_r (eV)	Width Γ (eV)
[2/1]	1.217	0.150
[3/1]	1.216	0.152
[3/2]	1.216	0.150
[4/2]	1.216	0.151
[4/3]	1.216	0.151

TABLE II. Resonance parameters of the ${}^2\Pi_u$ negative ion state of diacetylene calculated at various displacements $\Delta R_{C\equiv C}$ from the equilibrium distance $R_{C\equiv C} = 1.215$ Å. The calculation was performed at the PA [3/1] level.

$\Delta R_{C\equiv C}$ (Å)	Energy (eV)	Width (eV)
-0.18	2.324	1.040
-0.16	2.284	0.702
-0.14	2.180	0.543
-0.12	2.020	0.471
-0.10	1.880	0.433
-0.08	1.747	0.360
-0.05	1.552	0.260
-0.04	1.484	0.236
-0.02	1.323	0.179
-0.01	1.258	0.158
0.00	1.216	0.152
+0.01	1.148	0.137
+0.02	1.078	0.125
+0.04	0.943	0.099
+0.05	0.877	0.088
+0.08	0.680	0.060
+0.10	0.552	0.043
+0.12	0.428	0.030
+0.14	0.309	0.018
+0.18	0.087	0.003

for ${}^2\Pi_u$ state of the negative ion (red curve). The ground state ${}^1\Sigma_g$ curve and the bound state section of ${}^2\Pi_u$ state of negative ion were calculated with the same parameters as described in Section IV. As a practical note to application of the RAC method, we observed that the best fit is obtained at internuclear distances close to the equilibrium and the quality of the fit deteriorates with increasing distance from the equilibrium.

In Table III, we attempt to summarize available results that are connected with the ${}^2\Pi_u$ resonance. First two rows of the table can be directly compared with the present calculations

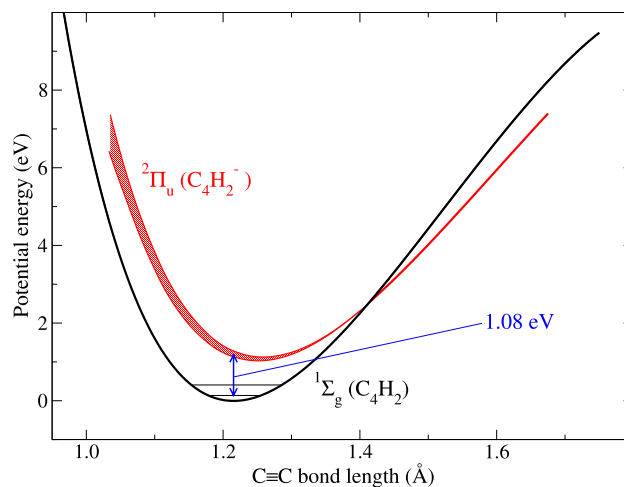


FIG. 3. Potential energy curve for the ground state ${}^1\Sigma_g$ of the neutral diacetylene molecule (black curve) is shown as a function of $C\equiv C$ bond length distance. Potential energy curve for ${}^2\Pi_u$ state of the negative ion is displayed by red curve. Vertical width of the red curve in the autodetachment region shows the width Γ of the resonance. Blue arrow indicates an energy of observed resonant peak in vibrationally inelastic cross sections obtained as vertical affinity lowered by zero point vibration.

TABLE III. Comparison of available results for the ${}^2\Pi_u$ resonance of diacetylene with the present calculations at the equilibrium geometry. Not all of the reported data can be directly compared with the present results. See details in the text.

Origin of the results	Energy (eV)	Width (eV)	
Fixed nuclei theory ¹⁹	0.47	0.065	
Fixed nuclei theory ²⁰	2.2	0.300	Width reported as $\Gamma/2$
Vibrational theory ¹⁸	1.33	~ 0.32	Estimated peak width
Vibrational experiment ¹⁷	1.01	~ 0.50	Published peak width
Present theory (aug-cc-pVTZ)	1.216	0.152	
Present theory (aug-cc-pVQZ)	1.166	0.156	

as the reported data represent fixed nuclei resonance positions and widths derived from scattering calculations.

The resonance parameters obtained from vibrationally inelastic calculations and experiments (third and fourth rows of Table III) are more difficult to compare with. In particular, the resonant peak observed in the experimental cross section for excitation of the C \equiv C stretch mode¹⁷ (positioned at 1.01 eV) exhibits a boomerang structure with the boomerang spacing corresponding to the C—H bend mode of the negative ion. This indicates that the ${}^2\Pi_u$ resonance efficiently couples these two vibrational modes and they cannot be treated separately. Moreover, we believe that the peak position observed in the vibrationally inelastic collisions corresponds to the energy shown by the blue arrow in Fig. 3, i.e., observed resonance position is lower than the vertical affinity by the zero point vibration. Hence, our calculations predict the inelastic peak at 1.08 eV.

The width observed in the vibrationally inelastic cross-section peak represents a joint effect of Frank-Condon width and the resonance (autodetachment) width. Therefore, we estimate that the widths listed in the third and fourth rows of Table III form an upper bound for the autodetachment width calculated in the present paper. For the sake of completeness, it is necessary to mention that the observed width of narrower boomerang peaks (~ 30 meV) seen in the experiment¹⁷ was also reported as the autodetachment width of the ${}^2\Pi_u$ resonance.

VI. CONCLUSIONS

We propose a remarkably simple method for calculation of low-lying molecular shape resonances (transient negative ions). This RAC method is a variant of the known method of analytical continuation in the coupling constant but, owing to the physical constraints imposed on the continued function, it is considerably more stable and robust. Even the lowest PA [2/1] yields reasonable estimates of resonance energy and width for common polyatomic molecules. Our experience shows that the present method is suitable for resonances for which the width Γ is smaller than the energy E (say $\Gamma < E/4$). For broad resonances where the width is comparable to the resonance energy, the obtained results are less satisfactory.

Results presented in the paper make use of the external Coulomb field, although the RAC theory is developed strictly for short-range perturbation potentials. We demonstrate that such a contradiction is partially solved by a finite support

of basis functions employed in practical implementations of methods used in quantum chemistry. Computed affinities are plagued by the presence of Rydberg states at low energies and they must be removed before the analytical continuation procedure.

Since the RAC method is based on the analytical continuation of affinities for a bound-state system, it is independent of the correlation model employed for the many-electron Hamiltonian. This allowed us to employ CCSD-T method to determine resonance parameters of the ${}^2\Pi_u$ state of diacetylene. While present results do not confirm any of the previous theoretical findings for fixed-nuclei resonance parameters, we obtained very good agreement with the experimental¹⁷ and the theoretical¹⁸ data for electron-impact vibrational excitation of diacetylene. In the case of the resonant position, the discrepancy between present aug-cc-pVTZ results and the experiment is about 70 meV. Our preliminary results indicate that this difference can be attributed to inaccurate representation of the correlation energy by the aug-cc-pVTZ basis set (aug-cc-pVQZ preliminary results and the experiment differ by ~ 20 meV). Moreover, it appears that the ${}^2\Pi_u$ resonance couples the C \equiv C stretch and C—H bend modes with boomerang oscillations along the C—H bend mode. Therefore, the judgement on the computed resonance width may require a nuclear dynamics simulation along at least two nuclear coordinates.

The main aim of this paper was to describe the new method and to demonstrate that it can provide reasonable values of resonance energies and widths for polyatomic molecules. In our next paper, we will consider more details of the method and its application to other polyatomic molecules.

ACKNOWLEDGMENTS

We acknowledge the funding by the Grant Agency of the Czech Republic (Grant No. P208/11/0452) and by the Czech Ministry of Education and Youth (Grant No. LD14088).

¹A. J. F. Siegert, *Phys. Rev.* **56**, 750 (1939).

²V. I. Kukulin, V. M. Krasnopolsky, and J. Horáček, *Theory of Resonances: Principles and Applications* (Kluwer Academic Publishers, Dordrecht, Boston, London, 1988).

³N. Moiseyev, *Phys. Rep.* **302**, 211 (1998).

⁴V. I. Kukulin and V. M. Krasnopolsky, *J. Phys. A: Math. Gen.* **10**, L33 (1977).

⁵V. M. Krasnopolsky and V. I. Kukulin, *Phys. Lett. A* **69**, 251 (1978).

⁶J. Horáček, P. Mach, and J. Urban, *Phys. Rev. A* **82**, 032713 (2010).

⁷P. Papp, Š. Matejčík, P. Mach, J. Urban, I. Paidarová, and J. Horáček, *Chem. Phys.* **418**, 067301 (2013).

⁸J. Horáček, I. Paidarová, and R. Čurík, *J. Phys. Chem. A* **118**, 6536-6541 (2014).

⁹T. Sommerfeld and M. Ehara, *J. Chem. Phys.* **142**, 034105 (2015).

¹⁰G. A. Baker and P. Graves-Morris, *Padé Approximants* (Addison-Wesley Publishing Co., 1981).

¹¹D. Bessis, *J. Comput. Appl. Math.* **66**, 85 (1996).

¹²D. E. Shemansky, A. I. F. Stewart, R. A. West, L. W. Espito, J. T. Hallet, and X. Liu, *Science* **308**, 978 (2005).

¹³M. Burgdorf, G. Orton, J. van Cleve, V. Meadows, and J. Houck, *Icarus* **184**, 634 (2006).

¹⁴X. Gu, Y. Guo, A. M. Mebel, and R. I. Kaiser, *Combust. Flame* **151**, 245 (2007).

¹⁵A. D'Anna, M. Alfe, B. Apicella, A. Tregrossi, and A. Ciajolo, *Energy Fuels* **21**, 2655 (2007).

¹⁶M. Allan, *Chem. Phys.* **86**, 303 (1984).

- ¹⁷M. Allan, O. May, J. Fedor, B. C. Ibanescu, and L. Andric, *Phys. Rev. A* **83**, 052701 (2011).
- ¹⁸R. Čurík, I. Paidarová, M. Allan, and P. Čársky, *J. Phys. Chem. A* **118**, 9734 (2014).
- ¹⁹M. Allan, C. Winstead, and V. McKoy, *Phys. Rev. A* **83**, 0062703 (2011).
- ²⁰I. Baccarelli, F. Sebastianelli, B. M. Nestmann, and F. A. Gianturco, *Eur. Phys. J. D* **67**, 93 (2013).
- ²¹P. J. Knowles, C. Hampel, and H.-J. Werner, *J. Chem. Phys.* **99**, 5219-5227 (1993); Erratum, **112**, 3106 (2000).
- ²²M. J. O. Deegan and P. J. Knowles, *Chem. Phys. Lett.* **227**, 321 (1994).
- ²³H.-J. Werner, P. J. Knowles, G. Knizia, F. R. Manby, M. Schutz *et al.*, MOLPRO, version 2010.1, a package of *ab initio* programs, 2010, see <http://www.molpro.net>.
- ²⁴T. H. Dunning, Jr., *J. Chem. Phys.* **90**, 1007 (1989).
- ²⁵R. Tay, G. F. Metha, F. Shanks, and D. McNaughton, *Struct. Chem.* **6**, 47 (1995).
- ²⁶O. May, J. Fedor, B. Ibanescu, and M. Allan, *Phys. Rev. A* **77**, 040701(R) (2008).
- ²⁷M. J. Seaton, *Rep. Prog. Phys.* **46**, 167 (1983).